# Structural and electronic properties of crystalline and molten Zintl phases: The Li-Ga system

J. Hafner and W. Jank
*Institut für Theoretische Physik, Technische Universität Wien, Wiedner Hauptstrasse 8/10, A-1040 Wien, Austria*
(Received 3 June 1991)

We present a theoretical investigation of the structural and electronic properties of crystalline and molten Li-Ga alloys. The atomic structure of the liquid phases is determined by molecular dynamics, based on pseudopotential-derived interatomic forces. The electronic structure is calculated using the linear-muffin-tin-orbital (LMTO) method for the crystalline compounds LiGa, $Li_3Ga_2$, and $Li_2Ga$, and using an LMTO-supercell approach for several liquid alloys. Our results demonstrate the validity of an extended Zintl principle. The bonding is dominated by the attractive potential of the Ga ions and may be described at least formally in terms of an electron transfer from Li to Ga. The atomic structure of the Ga sublattice in the crystalline compounds and the short-range Ga-Ga correlations in the melt, as well as the electronic structure, are found to be Ge-, As-, and Se-like with increasing Li concentration and an increasing number of electrons per Ga atom.

## I. INTRODUCTION

Since their discovery by Zintl and co-workers,[1] the intermetallic compounds of the alkali metals with the polyvalent elements from groups IIIB to VB of the Periodic Table have attracted the interest of physicists and chemists because of their outstanding structural and electronic properties. Intuitively, one would expect a predominantly ionic bond as a consequence of the large electronegativity difference between the constituent elements. However, it was pointed out already by Zintl[1] that the real structures are far more complex: many of the stable phases have no simple anions, but rather polyanionic clusters or infinite anion sublattices. The atomic arrangement in these anionic complexes corresponds to the element having the same number of valence electrons.[2] Hence, at least three different types of compounds are encountered in these systems:[3] saltlike compounds, polyanionic cluster compounds, and intermetallic phases. Recent investigations have demonstrated that the saltlike and the clustered compounds exist even in the liquid state.[4] Evidence comes from electronic transport measurements[5,6] that indicate a transition from a metallic conductivity to a semiconducting behavior in a narrow concentration range around the composition of the compound, and from diffraction experiments[7–9] that demonstrate that the local order is very similar in the crystalline and in the liquid phases. Further evidence comes from thermodynamic investigations.[10] For the theorist, the challenge is to explain the structure and the bonding properties of the crystalline phases, and to predict which of these phases will also exist in the liquid state. This paper is the first in a series devoted to this problem.

The situation is relatively clearcut for alloys of the alkali metals with a tetravalent element. All three types of compounds are found: Saltlike compounds close to the octet composition $A_4X$ ($A$ = alkali metal, $X$ = Si, Ge, Sn, or Pb) are the most stable phases in the Li-$X$ system. Electronic-structure calculations[11] show that a narrow gap separates the occupied anion bands from the lowest empty cation band. Equiatomic cluster compounds $AX$ with $X_4^{4-}$ tetrahedra are the most stable compounds formed by the heavy alkali metals K, Rb, and Cs (note that, according to the Zintl principle,[1] the $X_4^{4-}$ clusters are isoelectronic and isomorphic to the pnictide molecules). For these compounds, the Fermi level falls into a gap which originates from the splitting of bands which are bonding and antibonding within the anion tetrahedra,[11–13] and this explains their semiconducting behavior. Finally, there are also Pb-rich metallic compounds with crystal structures dominated by geometrical packing requirements (e.g., $NaPb_3$: $AuCu_3$ type, $KPb_2$: $MgCu_2$ type). The octet and cluster compounds also exist in the liquid state.[7,8,14,15] This indicates that the iono-covalent bonding properties are largely unaffected by the breakdown of translational symmetry.

The alloys of the alkali metals with the pentavalent elements show a more complex behavior. Again, one finds the three types of compounds postulated by Klemm:[3] saltlike $A_3X$ compounds with the $BiF_3$ and $AsNa_3$ structures, equiatomic cluster compounds $AX$ with either the LiAs or the NaP crystal structure (here the polyanionic clusters are spiral chains of pnictide ions corresponding to the chains in trigonal Se and Te), and metallic compounds $AX_2$ typically with a Laves phase structure (see, e.g., Villars and Calvert[16] and Schnering *et al.*[17]). The electronic properties of the octet compounds[18,19] conform with the picture of charge-transfer compounds which works so well for the I-IV compounds. In the liquid phase, the stable octet compounds formed by Li, Na, K, and Rb with Bi, and by Cs with Sb persist in the liquid state,[6,20,21] but there is no indication for a liquid compound corresponding to crystalline $Cs_3Bi$. In liquid Cs-Bi, a metal-nonmetal transition occurs at a composition of 40 at. % Bi, and strong conductivity anomalies at this

 

composition are also observed in liquid Rb-Bi and K-Bi alloys.[21,22] The metal-nonmetal transition at 40 at. % Bi has been attributed to the formation of broken Bi chains: thermal disorder breaks the infinite chains that exist in the crystalline cluster compounds and excess alkali atoms are needed to provide the electrons necessary to saturate the dangling bonds of a chain segment.[9,20,21] Such chain segments could also exist in the structurally unresolved $A_3X_2$ and $A_5X_4$ compounds. Hence, the simple picture of structures persisting through the melting point, which is so useful in rationalizing the properties of the liquid I-IV alloys, seems to break down here. The reason is probably that infinitely extended polyanionic chains cannot subsist in the liquid phase.

A similar situation has to be expected for the alloys of the alkali metals with the group-III elements. Here the difference in valence is too small to stabilize an octet compound. According to the Zintl principle, the cluster compound has an infinite anion sublattice which is isostructural and isoelectronic to the diamond lattice of the elemental semiconductors. Modern electronic structure calculations largely support Zintl's[1,23] and Hückel's[24] conjectures of a covalent $sp^3$-type bond between the trivalent metal atoms.[25–27] However, the large volume contractions observed for the I-III Zintl phases ($\Delta V=-29\%$ for LiGa, $\Delta V=-15\%$ for LiAl) should serve as a caveat that this is not simply an ordinary covalent bond. The question is then whether the atomic arrangement in the liquid is also dominated by the covalency of the bond. For the elemental and compound semiconductors it is known that melting destroys the $sp^3$ hybrids in the case of the elements and III-V compounds (the liquid phase is metallic with a free-electron-like density of states at the Fermi level),[28–31] whereas the II-VI compounds show a tetrahedral coordination even in the liquid state.[32] Recently several physical properties of molten I-III alloys have been investigated. Knight-shift and magnetic-susceptibility measurements indicate a substantial charge transfer.[33,34] Resistivity values of the liquid alloys of Li or Na with group-III metals are compatible with a free-electron regime, whereas alloys of (K, Rb, Cs) with group-III elements are definitely within the strong-scattering regime.[33,35] Diffraction experiments have been performed only for liquid Li-Ga (Ref. 36) and for Na-Tl (Ref. 37) alloys. The results show a pronounced prepeak whose position relative to the main peak is intermediate between that found in octet and in cluster compounds. The prepeak is more intense in the alkali-metal-rich range than at equiatomic composition[37]—again this is not directly compatible with a short-range order in the liquid that is directly related to the structure of the crystalline Zintl compound.

In this paper we present a theoretical investigation of the structural and electronic properties of crystalline and liquid I-III alloys using as an example the Li–Ga system. We report self-consistent electronic-structure calculations for the crystalline intermetallic compounds, molecular-dynamics simulations of the atomic structure of the liquid alloys (based on interatomic interactions deduced from pseudopotential theory), and supercell calculations of their electronic structure.

## II. ELECTRONIC STRUCTURE AND BONDING IN CRYSTALLINE Li-Ga COMPOUNDS

### A. Phase diagram and crystal structures

The phase diagram of the Li-Ga system as determined by Itami *et al.*[38] is shown in Fig. 1. The five intermetallic compounds fall into two distinctly different classes: The Zintl-phase LiGa and the Li-rich compounds $Li_3Ga_2$ and $Li_2Ga$ crystallize in ordered variants of a distorted body-centered-cubic packing[39,40] (the crystallographic data are summarized in Table I), with eight nearest and six next-nearest neighbors. In $Li_2Ga$ each Ga atom has two nearest Ga neighbors at a distance of $d=2.632$ Å. The Ga atoms form infinite zigzag chains with a bond angle of $\theta=112.6°$ [Fig. 2(a)]. In $Li_3Ga_2$, each Ga atom has three like neighbors at $d=2.674$ Å. The Ga chains of the $Li_2Ga$ structure are now linked in such a way that the Ga atoms form layers of puckered six-membered rings with a Ga-Ga-Ga bond angle of $\theta=109.5°$ [Fig. 2(b)]. In the NaTl-type LiGa phase, these six-membered rings are finally joined together in such a way that the diamond-type sublattice of Ga is formed [Fig. 2(c)]. The Ga-Ga distance in the Zintl phase is $d=2.663$ Å, the bond angle of $\theta=109.5°$ is the same as in the $Li_3Ga_2$ phase. Ga zigzag chains are also found in the metastable $\beta$ phase of Ga formed by crystallization from the supercooled melt.[41] Note that the intrachain distances in $\beta$-Ga ($d=2.688$ Å, $\theta=103.4°$) are larger than in any of the Li-Ga compounds. The short Ga-Ga distances, together with the large volume contraction ($\Delta V$ varies between $-24\%$ and $-29\%$, see Table I) is a hint to strong chemical bonding effects in these compounds.

The Ga-rich compounds are of an entirely different character. Like many alloys of Ga with the heavy alkali metals ($AGa_7$, $A$=Rb, Cs; $AGa_3$, $A$=K, Rb), $Li_3Ga_{14}$ contains Ga icosahedra.[42] In $Li_3Ga_{14}$, each icosahedron is directly linked to six adjacent homologs and the

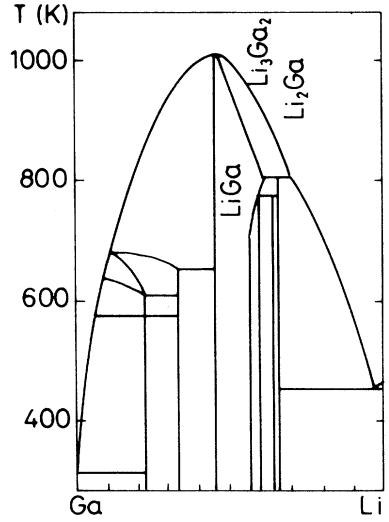


FIG. 1. Li-Ga phase diagram (after Itami, Shimoji, and van der Lugt, Ref. 38).

TABLE I. Crystallographic description of the bcc-based Li-Ga phases.

| $Li_2Ga$[a] | | | | | |
|---|---|---|---|---|---|
| Space group $D_{2h}^{17}$-$C_{mcm}$ | | | Atomic positions | | |
| $a=4.562$ Å | Ga | (4c) | 0 | 0.0763 | $\frac{1}{4}$ |
| $b=9.542$ Å | Li(1) | (4c) | 0 | 0.757 | $\frac{1}{4}$ |
| $c=4.364$ Å | Li(2) | (4c) | 0 | 0.412 | $\frac{1}{4}$ |
| Atomic volume $V_{at}=15.83$ Å | | | | | |
| Excess volume $\Delta V_{at}=-23.9\%$ | | | | | |
| $Li_3Ga_2$[a] | | | | | |
| Space group $D_{3d}^{5}$-$R\bar{3}m$ | | | Atomic positions | | |
| $a=4.367$ Å | Ga | (6c) | 0 | 0 | 0.8013 |
| $c=13.896$ Å | Li(1) | (3a) | 0 | 0 | 0 |
| | Li(2) | (6c) | 0 | 0 | 0.405 |
| Atomic volume $V_{at}=15.30$ Å$^3$ | | | | | |
| Excess volume $\Delta V_{at}=-26.0\%$ | | | | | |
| LiGa[b] | | | | | |
| Space group $O^h$-$Fd\bar{3}m$ | | | Atomic positions | | |
| $a=6.150$ Å | Ga | (8a) | 0 | 0 | 0 |
| | Li | (8b) | $\frac{1}{2}$ | $\frac{1}{2}$ | $\frac{1}{2}$ |
| Atomic volume $V_{at}=14.53$ Å$^3$ | | | | | |
| Excess volume $\Delta V_{at}=-29.0\%$ | | | | | |

[a]After Ref. 39.
[b]After Ref. 19.

remaining vertices are connected to neighboring icosahedra via isolated Ga atoms. Hence, Ga is six-coordinated with five neighbors forming a flat pentagonal pyramid and one extra perpendicular bond, as in the icosahedral structure of $\alpha$-boron[43] (note that there is also a $Li_3B_{14}$ compound with a structure closely related to $Li_3Ga_{14}$).

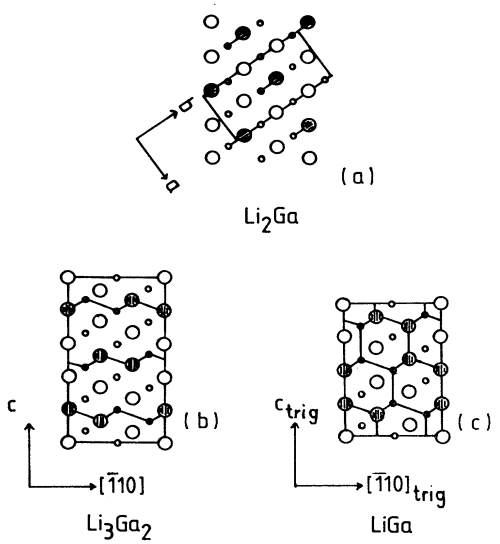


FIG. 2. Comparative view on the crystal structures of (a) $Li_2Ga$ (b) $Li_3Ga_2$, and (c) LiGa. Solid circles, Ga; open circles, Li. Large circles represent atoms in the plane, smaller circles atoms above or below the plane. After Müller and Stöhr, Ref. 39.

Unlike the Li-rich compounds, $Li_3Ga_{14}$ shows only a modest volume contraction of $\Delta V=-3.8\%$ (Table II).

### B. Electronic structure

We have performed self-consistent electronic structure calculations for the Li-Ga compounds using the linearized muffin-tin-orbital method in the atomic sphere approximation (LMTO-ASA).[44,45] We used a scalar relativistic wave equation, exchange and correlation are described by the local density-functional parametrization of von Barth, Hedin, and Janak.[46] The Brillouin-zone integrations for the electronic density of states (DOS) have been performed using the linear tetrahedron technique.[47] The total, partial, and angular-momentum-decomposed densities of state for LiGa in the NaTl structure are shown in Fig. 3(a). As in previous calculations for NaTl-type Zintl phases,[25–27] we obtain a Ge-like DOS with a deep minimum close to the Fermi level, indicating a high degree of $sp^3$ hybridization on the Ga sites. Pawlowska *et al.*[48] have shown that the bond order (equal to the difference in the number occupied bonding and antibonding orbitals) is a quantitative measure of the degree of $sp^3$ bonding. For the I-III Zintl phases they find bond orders between 0.48 and 0.58, to be compared with an $sp^3$ bond order of 0.68 for crystalline Si. For comparison we also show the DOS for a hypothetical CsCl-type phase of LiGa (the CsCl lattice is predicted to be the high-pressure polymorph of the I-III Zintl phases[26,27]). In this case, we find a high density of states at the Fermi level and a valence band that splits neatly in a lower part dominated by Ga $s$ states and an upper part dominated by Ga $p$

TABLE II. Crystallographic description of the $Li_3Ga_{14}$ phase. The asterisk indicates an occupation probability of 50%.

| Space group $D_{3d}^5$-$R\bar{3}m$ | | Atomic positions | | | |
|---|---|---|---|---|---|
| $a=8.441$ Å | Ga(1) | (6c) | 0 | 0 | 0.8224 |
| $c=16.793$ Å | Ga(2) | (18h) | 0.1608 | 0.8392 | 0.8646 |
| | Ga(3) | (18h) | 0.5611 | 0.4389 | 0.9485 |
| | Li | (18h)* | 0.8229 | 0.1771 | 0.0580 |
| Atomic volume $V_{at}=20.32$ Å$^3$ | | | | | |
| Excess volume $\Delta V_{at}=-3.8\%$ | | | | | |

states. The DOS at the Li sites shows a completely mixed angular-momentum character in both structures. This means that the electronic structure is dominated by the strong attractive Ga potential. It does not mean, however, that there is a complete charge transfer from the atomic spheres centered at the Li sites to those centered at the Ga atoms. The valence charge densities are not zero, nor even small within the Li spheres. It only indicates that the valence bond states originate from the atomic Ga states, hybridized through the interaction with neighboring Ga states and shifted by the potential of the Li ions. The change in the crystal structure affects only the way in which the Ga states interact but not the fact that the valence DOS is entirely dominated by the anion states.

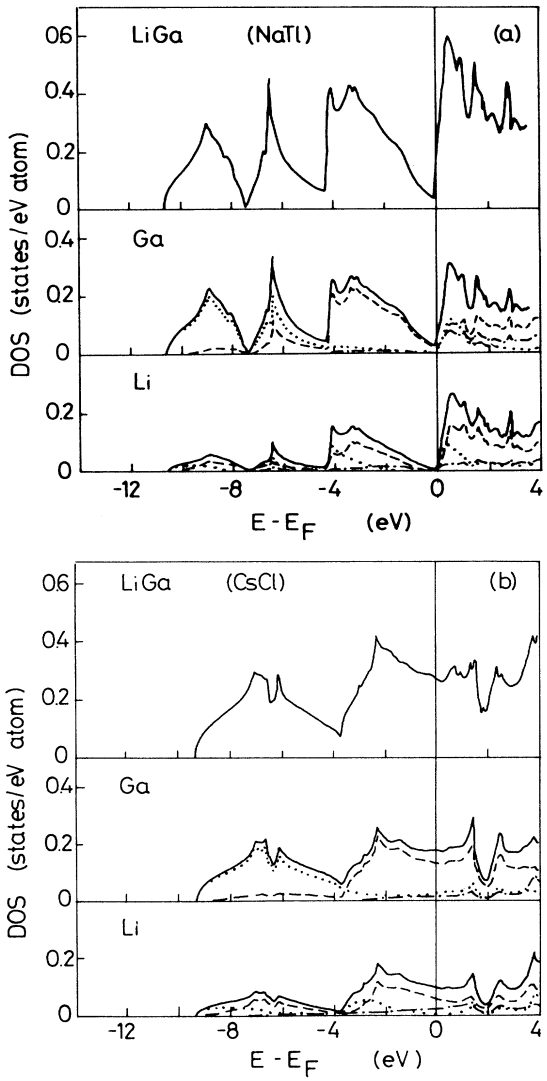


FIG. 3. Total, partial, and angular-momentum-decomposed electronic density of states for LiGa in the (a) NaTl and (b) CsCl structures. Solid line, total DOS; dotted line, *s*-DOS; dashed line, *p*-DOS; dot-dashed line, *d*-DOS.

The valence DOS for $Li_3Ga_2$ is shown in Fig. 4. Again the valence band is split in three parts, but now the two lowest bands are entirely of Ga *s* character, each contains exactly one electron per Ga atom. The third band is a Ga *p* band, up to the pseudogap about 1 eV above the Fermi level it accommodates three electrons per Ga atom. This means that the structure of the valence DOS of $Li_3Ga_2$ is strikingly similar to that of trigonal and rhombohedral As.[18] The $s^2p^3$ configuration of As leaves

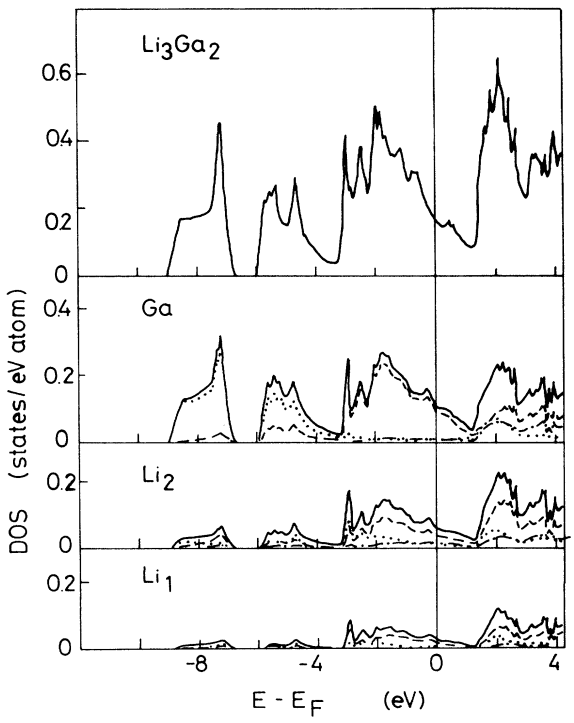


FIG. 4. Total, partial, and angular-momentum-decomposed electronic density of states for $Li_3Ga_2$. Key, see Fig. 3.

nonbonding $s$ electrons and one electron per $p$ orbital. Simple-cubic As with undistorted ($pp\sigma$) bonds would have a half-filled metallic $p$ band, but is unstable against a Peierls distortion. The distortion splits both the $s$ and the $p$ band, and both rhombohedral and orthorhombic As are semimetallic. Although, even assuming a complete electron transfer from Li to Ga, the electron configuration of Ga in $Li_3Ga_2$ is only $s^2p^{2.5}$, the same Peierls distortion mechanism determines the crystalline lattice and the valence-band structure. The Ga layers of puckered six-membered rings may be considered as being derived from a simple-cubic Ga sublattice by a bond-breaking distortion. The gap in the $s$ band is characteristic for a structure with only even-membered rings. Of course, the potential of the Ga ions is much weaker than that of the As ions, so one would expect the lattice distortion to be weaker. On the other hand, the Li ions intercalated between the Ga layers reduce the influence of Ga-Ga backbonds (note that Ga ions that are not nearest neighbors, are only third-nearest neighbors in LiGa, $Li_3Ga_2$, and $Li_2Ga$) so that a quite large lattice distortion results.

A similar picture arises from the DOS of $Li_2Ga$ (Fig. 5). The lowest band has Ga $s$ character, it contains two electrons per Ga atom. The form of the DOS is characteristic for a one-dimensional band with ($ss\sigma$) bonds. The second band is predominantly of Ga $p$ character. Up to the DOS minimum, about 1.7 eV above the Fermi energy, this band contains four states per Ga atom, out of which three states are occupied. This shows that there is at least some similarity between the electronic structure of $Li_2Ga$ and that of trigonal Se and Te. However, the analogy should not be stressed too far. The characteristic splitting of the $p$ band in trigonal Se into bonding, nonbonding, and antibonding bands is absent in $Li_2Ga$. As shown by Ikawa and Fukutome,[49] the structure of the Se $p$ band is strongly correlated with the helical form of the Se chains. The helical structure is found to be stabilized by the interaction of the lone pair of electrons in the nonbonding band with adjacent ($pp\sigma$) bonds. In the $Li_2Ga$ structure with planar Ga zigzag chains the detailed structure of the $p$ band is missing.

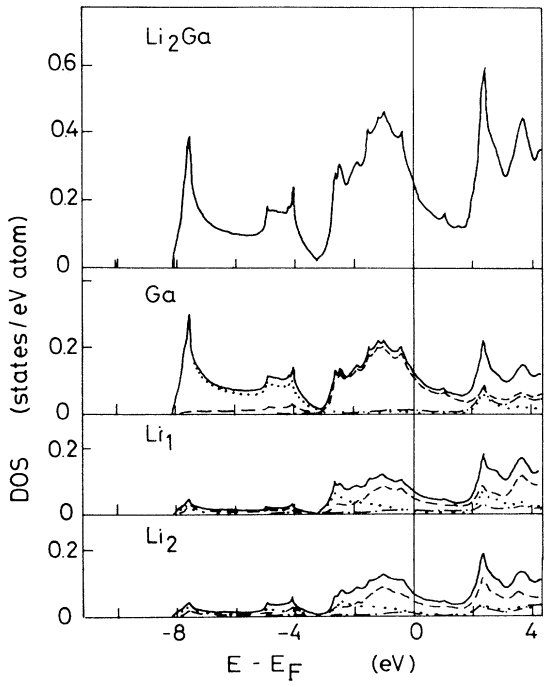


FIG. 5. Total, partial, and angular-momentum-decomposed electronic density of states for $Li_2Ga$. Key, see Fig. 3.

An important point is also that all Li-Ga compounds (and the corresponding Li-Al compounds) are formed at an appreciable electron deficit relative to the idealized reference system. This includes the equiatomic NaTl-type I-III phases which always contain about 4% vacancies on the Li sites[50] corresponding to an electron deficit of 4% and the NaTl-type I-II phases LiZn and LiCd which form $sp^3$ hybrids at an electron deficit of 25%. In $Li_3Ga_2$ the electron deficit is 10%, in $Li_2Ga$ 16.6% relative to an ideal As-like, respectively, Se-like bonding configuration. This tendency to form polyanionic cluster compounds even if not all bonds are saturated is also found in other systems. The CrB structure with planar zigzag chains of B atoms, for example, is formed not only in the II-IV compounds of Ca, Sr, Ba, with Si, Ge, or Sn (where the $pp\sigma$ bonds forming the chains are saturated according to conventional electron-counting rules),[16] but also in the IIa-IIb compounds like CaZn, BaZn where the $pp\sigma$ band is only half-full.[51]

Very recently Guo *et al.* have investigated the electronic structure of LiAl, $Li_3Al_2$, and $Li_9Al_4$ using the full-potential linearized augmented-plane-wave method.[52] LiAl crystallizes in the NaTl structure, $Li_3Al_2$ is isotopic to $Li_3Ga_2$, the $Li_9Al_4$ structure is similar to that of $Li_2Ga$ and shows again zigzag chains of Al atoms (the relation between these structures has been discussed in detail by Müller *et al.*[39]). The electronic densities of state presented by Guo *et al.* are very similar to our results for the Li-Ga compounds. In addition, they present charge density plots for $Li_3Al_2$ and $Li_3Al_4$ which demonstrate very clearly the piling up of a covalent bond charge in the center of the Al-Al bonds (for the Zintl-phase LiAl the same conclusion had been reached before by Hafner and Weber[27] and by Christensen[26]). However, if we agree with Guo *et al.*[52] in that the bonding in all Li-Al and Li-Ga compounds is dominated by the strong potential of the polyvalent atoms and at least partially covalent III-III bonds, we disagree in the more detailed interpretation. Guo *et al.* note that "Al atoms tend to form tetrahedral diamondlike bonds due to the donation of electrons by Li." While this is basically correct, the structure of the electronic DOS clearly shows that, in the Li-rich compounds, the bonding is not diamondlike but becomes first As-like and then even Se-like. This conclusion is supported by the pronounced decrease of the degree of $sp^3$ hybridization with increasing Li content.

## III. INTERATOMIC INTERACTIONS

Effective interatomic potentials for Li-Ga alloys have been calculated using the optimized first-principles pseudopotential theory based on an expansion of the valence-electron states in terms of orthogonalized plane waves. It

is well known that the effective interatomic interactions varies on alloying via the variation of the electronic screening length, of the wavelength of the Friedel oscillations, and of the effective pseudopotential in the alloy. The most important aspects in the variation of the potentials are (i) the reduction of the effective diameter of the electropositive atom (here Li), and (ii) the increase of the amplitude of the Friedel oscillations in the interaction between the electronegative ions (here Ga), especially at short distances. The first point is related to the fact that, at an increased average electron density, the Coulomb repulsion between the Li ions is screened over shorter distances. The second point arises from the reduction of the Fermi wave vector on alloying of a polyvalent metal with another metal with a lower electron density: the pseudopotential matrix element $|w_{Ga}(2k_F)|$ setting the amplitude of the pair interaction increases with decreasing $k_F$. For a more detailed discussion see Refs. 53 and 54.

The substantial compressions of the Li pseudoatoms (as measured by the repulsive part of the effective Li-Li interactions) is, of course, directly related to the large negative volume of formation. It has been shown[55] that the volume of formation of *sp*-bonded alloys may be calculated with reasonable accuracy by pseudopotential perturbation theory, even in the lowest-order approximation (Fig. 6). For the LiGa phase, this first-order calculation predicts a volume of formation of $\Delta V=-18.6\%$; this result is not substantially changed by a full second-order calculation ($\Delta V=-19\%$) or by a self-consistent total energy calculation using the LMTO [$\Delta V=-19.7\%$ (Ref. 26)]. The experimental volume of formation for LiGa is $\Delta V=-29.0\%$, see Table I. For all other I-III Zintl compounds, both the first-order prediction and the self-consistent total energy calculation agree much better with experiment, e.g., LiAl: $\Delta V=-21.7\%$ (first order), $\Delta V=-16.6\%$ [LMTO (Ref. 26)], $\Delta V=-15.0\%$ [expt. (Ref. 19)]; NaTl: $\Delta V=-21.8\%$ (first order), $\Delta V=-22.2\%$ [LMTO (Ref. 26)], $\Delta V=-20.6\%$ [expt. (Ref. 19)]. In general, the simple first-order prediction for $\Delta V$ is too strongly negative for compounds with a strong covalent contribution to the bonding and too small for a strongly ionic compound. This would indicate that it is not covalency that is responsible for the discrepancy in $\Delta V$, but it is not clear why Li-Ga should be more ionic than other I-III alloys.

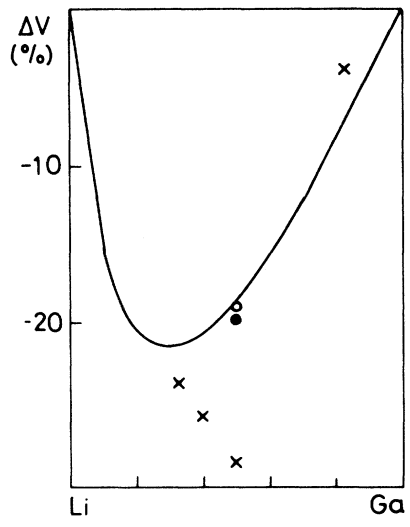


FIG. 6. Volume of formation $\Delta V$ of Li-Ga alloys. Solid line, first-order theory; open circle, second-order theory; solid circle, self-consistent LMTO total energy calculation; crosses, experiment.

The effective interatomic potentials for a series of crystalline and liquid Li-Ga alloys are shown in Fig. 7. These results illustrate (i) the substantial reduction of the effective repulsive diameter of the Li-Li pair interaction, (ii) a preferential interaction in unlike-atom nearest-neighbor pairs (the Li-Ga potential is stronger than the average of the Li-Li and Ga-Ga interactions), especially for Li-rich alloys, and (iii) the Ga-Ga potential which has nearly zero curvature around the nearest-neighbor distance in pure Ga, develops a distinct repulsive hump with increasing Li content of the alloy. This makes the Ga pair interaction similar to that of the elements with a higher valence (Ge, As, Se)—their pair potentials are shown for comparison in Fig. 7. Thus, we find that the similarity we found in the electronic structures is also reflected in the interatomic interactions.

This once again raises the question how a description in terms of quantum-mechanical pair and volume forces relates to the traditional description of open covalent structures in terms of localized bonds and bond charges.[56,57] In a series of recent publications[58–60] we have shown that the open, low-coordinated structures of liquid Si, Ge, As, Te, etc., are well described in terms of a modulation of a close-packed structure by the Friedel oscillations in the pair potential, and that this is essentially equivalent to a real-space formulation of the conventional picture of a Peierls distortion (which is usually formulated in reciprocal space[61]). Significant differences between the structures determined by the interplay of pair and volume forces and those calculated using the full set of quantum-mechanical many-body forces appear only at the level of four-body correlation functions.[62,63] For the crystals, pair and volume forces are sufficient to describe the static stability of the open relative to the close-packed structures, but not the dynamic stability: in this description the stiff bond-bending forces necessary for stabilizing certain shear modes are lacking. The reason is that second-order theory gives *sp* hybridized bonds describable in terms of overlapping spherical pseudoatoms.[64] It is covalency in the sense of metallic bonds with no directional properties and no limit to the number of bonds an atom can form beyond the limit set by packing requirements, i.e., the effective atomic size given by the repulsive diameter of the pair interactions and the atomic volume determined by the volume forces. True covalent bonding is describable only via higher-order corrections. The third-order corrections create a strong attractive potential which attracts an extra bonding charge to the bond site. The bond-bond interactions give the angular forces.

In a binary alloy the problem is more complicated: the pair forces must determine not only the nearest-neighbor topology, but also the chemical order—i.e., the relative

abundance of like- and unlike-atom pairs. The NaTl structure and the CsCl structure have the same bcc mean lattice, but in the NaTl structure each atom has four like and four unlike atoms, whereas in the CsCl structure each atom is surrounded by eight unlike neighbors. In LiGa (as in all I-III alloys), the pair forces prefer the formation of unlike-neighbor bonds at short distances. This is incompatible with the stability of the NaTl-type phases as long as only the nearest neighbors are considered. However, in the bcc lattice, the difference between first- and second-neighbor distances is only 15%, and both fall into the attractive well of the pair interactions. For the first- and second-neighbor shells together, there is an even more pronounced tendency to heterocoordination in the NaTl lattice (four like, ten unlike neighbors) than in the CsCl structure (six like, eight unlike neighbors). However, one finds that, to second-order in the pseudopotential, the CsCl structure is slightly more stable than the NaTl phase. It has been shown[65,66] that the leading third-order terms associated with the filling of the Jones zone of the NaTl structure must be included to get the correct phase stability. This reflects the relatively high degree of $sp^3$ hybridization.

In the Li-rich phases, the distortion of the bcc lattice mixes the first- and second-neighbor shell of the undistorted bcc lattice. In both the $Li_3Ga_2$ and $Li_2Ga$ structure, there is a strong preference for heterocoordination of the Ga sites (Table III), and a weak preference for unlike neighbors around the Li sites. This is just what corresponds to the form of the pair interactions (Fig. 7).

Thus, we find that the pair interactions of Li-Ga are reasonably well consistent with the crystal structures, except for some small covalent corrections which are necessary to understand the phase stability of LiGa. There, the situation is similar to that in the group-IV elements and we expect that, as in liquid Si and Ge, the pair interactions will yield a realistic description of the structure of liquid Li-Ga alloys.

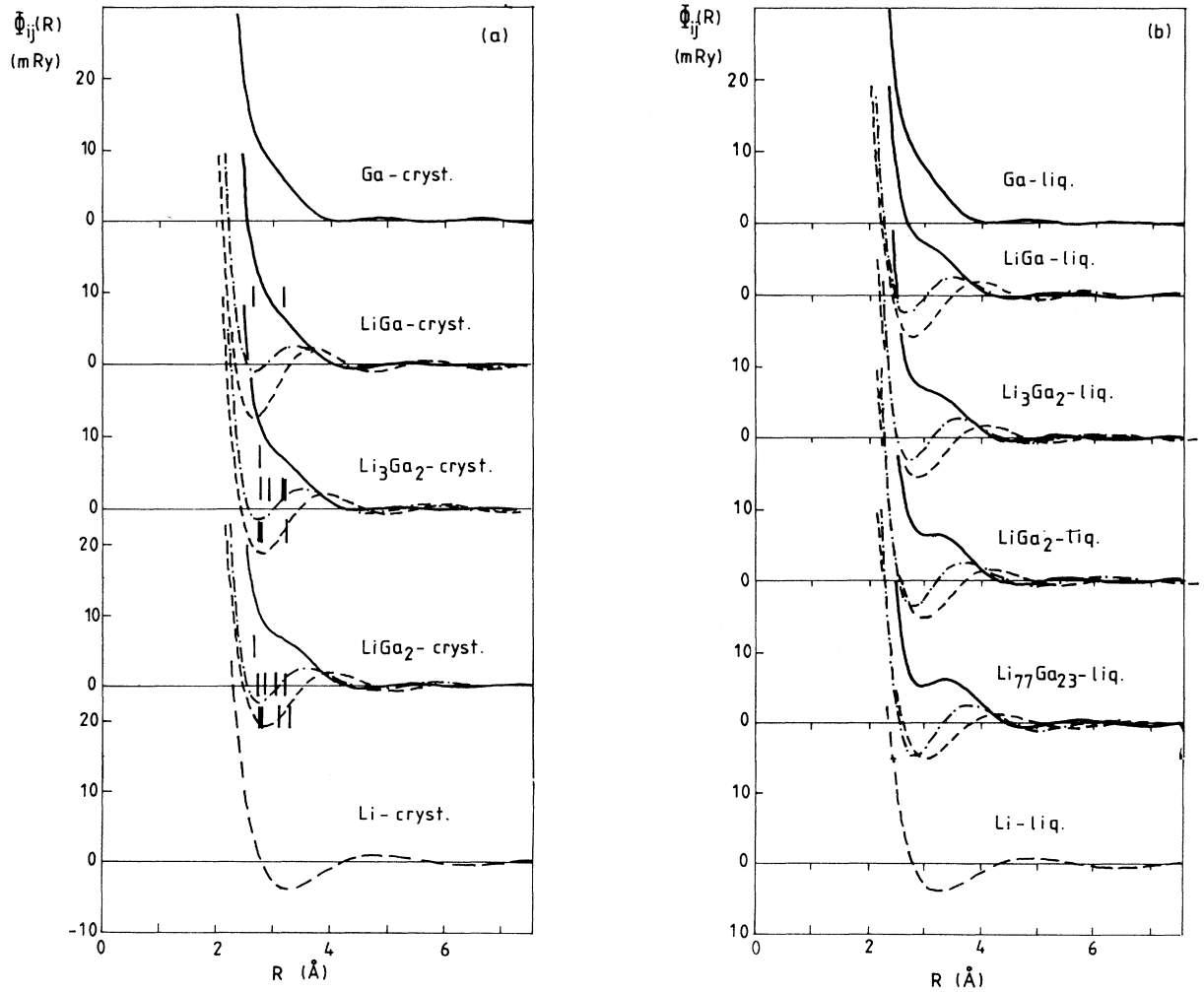


FIG. 7. Interatomic interactions in pure Li and Ga and in Li-Ga alloys (solid curve, Ga-Ga; dashed curve, Li-Li; dot-dashed curve, Ga-Li). The left column refers to the crystalline state, the middle column to the liquid state, the right column shows, for comparison, the pair interactions in Ge, As, and Se. The vertical bars mark the interatomic distances in the crystalline Li-Ga compounds. For LiGa the Li-Li, Li-Ga, and Ga-Ga distances are identical. For the $Li_3Ga_2$ and $Li_2Ga$ structures, the top row shows the Ga-Ga, the middle row the Li-Ga, and the lowest row the Li-Li distances.

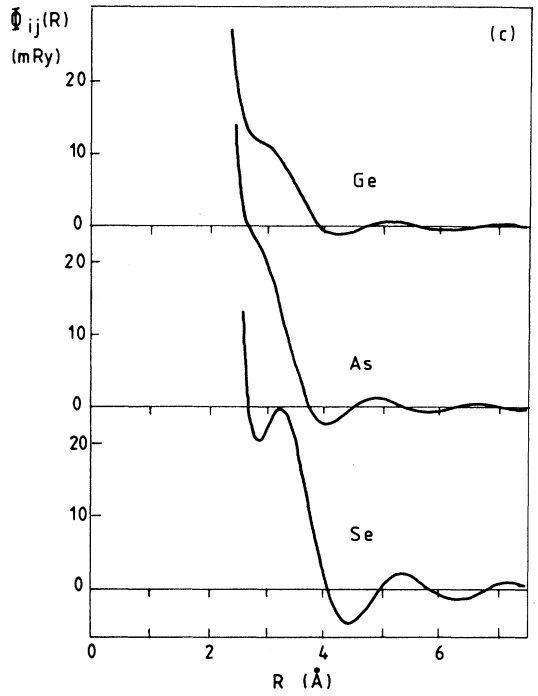


FIG. 7. (*Continued*).

## IV. LIQUID STRUCTURE

The structure of liquid Li-Ga has been calculated by microcanonical molecular dynamics, using the pair potentials described in Sec. III. Our molecular dynamics routine is based on a fourth-order predictor-corrector algorithm for the integration of the Newtonian equations of motion and an efficient network-cube algorithm for nearest-neighbor bookkeeping. For details see Refs. 58 and 67. For each alloy, two sets of simulation runs were done in parallel: one based on a large ensemble of $N=1000$ atoms and one for a small ensemble of $N=64$

TABLE III. Coordination numbers in crystalline Li-Ga compounds and liquid Li-Ga alloys. The numbers in parentheses give the partial coordination numbers for a random distribution of the chemical species.

| | | | Crystal | | | Melt[d] | | |
|---|---|---|---|---|---|---|---|---|
| | | | Li | Ga | tot | Li | Ga | tot |
| LiGa | a | Li | 4 | 4 | 8 | | | |
| | | | (4) | (4) | | | | |
| | | Ga | 4 | 4 | 8 | | | |
| | b | Li | 4 | 10 | 14 | 6.2 | 5.8 | 12.0 |
| | | Ga | 10 | 4 | 14 | 5.8 | 4.4 | 10.2 |
| | | | (7) | (7) | | (5.1) | (5.1) | |
| $Li_3Ga_2$ | c | Li | 6.66 | 7.33 | 14 | 7.9 | 5.4 | |
| | | Ga | 11 | 3 | 14 | 8.2 | 3.7 | 11.9 |
| | | | (8.4) | (5.6) | | (7.1) | (4.8) | |
| $Li_2Ga$ | c | 8 | 6 | 14 | 9.3 | 4.4 | 13.7 | |
| | | Ga | 12 | 2 | 14 | 9.0 | 2.7 | 11.7 |
| | | | (9.4) | (4.6) | | (7.8) | (3.9) | |
| $Li_{77}Ga_{23}$ | | Li | | | | 11.1 | 3.1 | 14.2 |
| | | | | | | (10.9) | (3.3) | |
| | | Ga | | | | 10.4 | 1.3 | 11.7 |
| | | | | | | (9.0) | (2.7) | |

[a]Nearest neighbors only.
[b]First and second neighbors.
[c]Averaged over crystallographically inequivalent Li sites.
[d]Calculated by integrating over the symmetric part of the first peak in the pair-correlation function.

atoms. The first set of simulations is used to create reliable pair correlation functions and structure factors for comparison with experiment, the second to produce the atomic coordinates for the electronic structure calculations.

It is rather difficult to determine the density of the liquid alloys to be used in the simulations. No accurate density measurements have been performed. In their analysis of the neutron-diffraction data, Reijers *et al.*[36] assume a density of $\rho=3.00$ g cm$^{-3}$ for LiGa, corresponding to an atomic volume of $V_{at}=21.37$ Å$^3$. This is equivalent to assuming a volume expansion of 47% at melting and can hardly be considered as a realistic estimate. In an attempt to model the diffraction data using correlation functions of a charged hard-sphere mixture calculated in the mean-spherical approximation, Reijers *et al.* found it necessary to use a much higher density of $\rho=3.59$ g cm$^{-3}$, which we consider as a more realistic estimate. For our calculations we started from the fact that the simple first-order prediction discussed in Sec. III is usually even more accurate for liquid than for crystalline alloys. For liquid Li-Pb alloys, for example, these predictions agree to within 2% with the experimental results.[68] Starting from the densities of the pure liquid metals, we arrive at the atomic volumes for the liquid alloys compiled in Table IV which we consider as a realistic estimate.

The partial pair correlation functions for Li-Ga alloys are shown in Fig. 8. We find that the Li-Li correlation functions correspond at all compositions rather closely to a random close-packed arrangement of the Li atoms, the ratio of the positions of the first and second peaks is $R_2/R_2\simeq 1.85-1.87$; i.e., rather close to the ideal hard-sphere value of $R_2/R_1=1.91$. The Ga-Ga correlations are entirely different: with increasing Li content, the first peak in $g_{\text{Ga-Ga}}(R)$ is strongly reduced, the number of Ga-Ga pairs is reduced from 4.4 in LiGa to 1.3 in $Li_{0.77}Ga_{0.23}$ and this is much lower than that which corresponds to a random distribution of the chemical species (see Table III). Note that these coordination numbers are very close to the Ga-Ga coordination numbers in the crystalline compounds. The Ga-Ga correlation functions are also strongly distorted, the ratio $R_2/R_1$ is now between $R_2/R_1=1.71$ and $R_2/R_1=1.60$, and this is close to the values characteristic of the correlation functions of the open structures of the liquid semimetals and semiconductors (see Table V). From the ratio $R_2/R_1$, we can directly calculate the predominant bond angle and the resulting values (between $\theta_{\text{Ga-Ga-Ga}}=117.5°$ in $Li_{0.5}Ga_{0.5}$ and $\theta_{\text{Ga-Ga-Ga}}=106°$ in $Li_{0.77}Ga_{0.23}$) are very close to those in the crystalline Li-Ga compounds ($\theta_{\text{Ga-Ga-Ga}}=109.5°$, 109.5°, and 112.6° in LiGa, $Li_3Ga_2$, and $Li_2Ga$, respectively). The total and partial bond-angle distribution functions are shown in Fig. 9. For $Li_{0.5}Ga_{0.5}$, the distribution of the bond angles is very similar around the Li and the Ga atoms: a broad distribution with two peaks close to $\theta\sim 50°-60°$ and $\theta\sim 100°-110°$ of about equal amplitude. This is similar to liquid Si and Ge.[28,29] At higher Li content, the 60° peak is reduced and at highest Li concentration $f_{\text{Ga-Ga-Ga}}(\theta)$ has a single peak close to the bond angle of the Ga zigzag chains in crystalline $Li_2Ga$.

At all compositions, the Li-Ga pair-correlation function has the highest amplitude. The partial coordination numbers determined by integrating over the first peak in the $g_{ij}(R)$'s (see Table III) show that at all compositions the coordination of the Li atoms is essentially random,

TABLE IV. Temperatures, atomic volumes, and volume contractions of the liquid Li-Ga alloys used in the MD simulations.

| | $T$ (K) | $\Omega_{at}$ (Å$^3$) | $\Delta\Omega$ (%) |
|---|---|---|---|
| $Li_{0.50}Ga_{0.50}$ | 1023 | 18.54 | −18.6 |
| $Li_{0.60}Ga_{0.40}$ | 1023 | 18.38 | −19.3 |
| $Li_{0.67}Ga_{0.33}$ | 873 | 18.26 | −19.5 |
| $Li_{0.77}Ga_{0.23}$ | 748 | 18.10 | −20.9 |

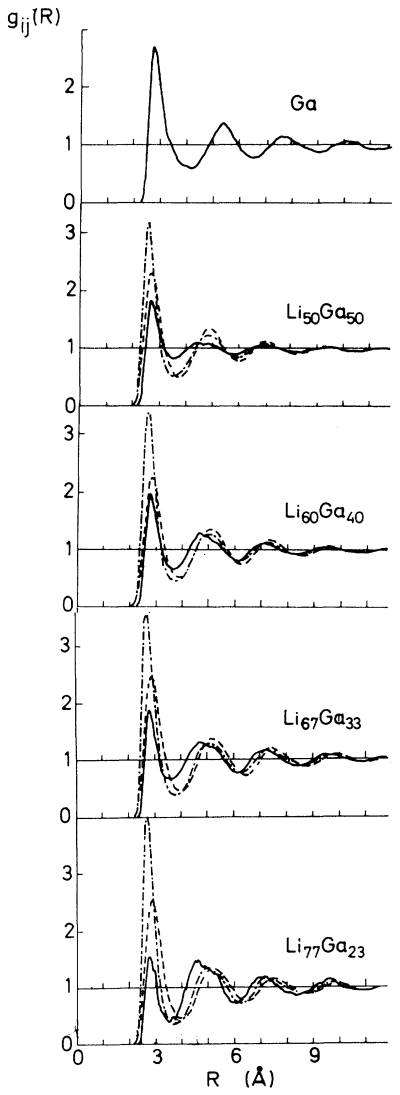


FIG. 8. Partial pair correlation functions $g_{ij}(R)$ in liquid Ga and liquid Li-Ga alloys. Solid line, Ga-Ga; dashed line, Li-Li; and dot-dashed line, Li-Ga correlations.

TABLE V. Ratio of the peak positions $R_2/R_1$, $Q_p/Q_1$, and $Q_2/Q_1$ in the correlation functions and structure factors of a hard-sphere like, of liquid Li-Ga alloys (partial Ga-Ga correlation function), and of liquid Ge, As, and Se.

| | $R_2/R_1$ | $Q_p/Q_1$ | $Q_2/Q_1$ | $Q_1/2k_F$ |
|---|---|---|---|---|
| Hard sphere | 1.91 | | 1.86 | |
| Liquid | | | | |
| $Li_{0.50}Ga_{0.50}$ | 1.71 | (0.75) | 1.75 | 0.97 |
| $Li_{0.60}Ga_{0.40}$ | 1.6 | 0.65 | 1.71 | 0.97 |
| $Li_{0.67}Ga_{0.33}$ | 1.67 | 0.66 | 1.73 | 0.99 |
| $Li_{0.77}Ga_{0.23}$ | 1.60 | 0.66 | 1.74 | 1.03 |
| | | $Q_1/Q_2$ | $Q_3/Q_1$ | $Q_2/2k_F$ |
| Ge[a] | 1.63 | (0.76) | 1.62 | 1.10 |
| As[b] | 1.49 | 0.66 | 1.50 | 1.04 |
| Se[c] | 1.52 | 0.60 | 1.51 | 1.06 |

[a]After Ref. 58.
[b]After Ref. 59.
[c]After Ref. 60.

whereas Ga sites are preferentially surrounded by Li atoms. The tendency to a Ga heterocoordination increases with the Li content of the alloy. This is again very similar to the chemical short-range order in the crystalline compounds. At concentrations between 65 and 75 at. % Li, the Ga-Ga coordination number is close to 2. This points to a chainlike substructure of the Ga atoms like $Li_2Ga$. From the bond-angle distribution we learn that even the chain angle is similar in the crystalline and in the liquid phase. Thus, the picture of the liquid structure of Li-Ga alloys emerging from the discussion of the real-space correlations is one of rather well-defined Ga clusters embedded in a randomly close-packed Li matrix. The structure of the Ga clusters resembles broken pieces of the Ga sublattices of the crystalline compounds.

This conjecture is further confirmed by the partial static structure factors [Fig. 10(a)]. The Li-Li structure factor is again close to the form expected for hard-sphere-like liquids. The Ga-Ga structure factor shows a strong prepeak at all Li concentrations beyond 50 at. % Li. The Li-Ga structure factor has a minimum at these momentum transfers. The prepeak in the Ga-Ga structure factor arises from both chemical and topological short-range ordering: in the Bhatia-Thornton structure factors [Fig. 10(b)] we find a small shoulder in the density-fluctuation structure factor $S_{NN}(q)$ (representing the average topological order) and a broad prepeak in the concentration-fluctuation structure factor $S_{CC}(q)$. The Ga-Ga structure factor is surprisingly similar to the structure factor of the liquid polyvalent semiconductors Ge, As, and Te: the ra-

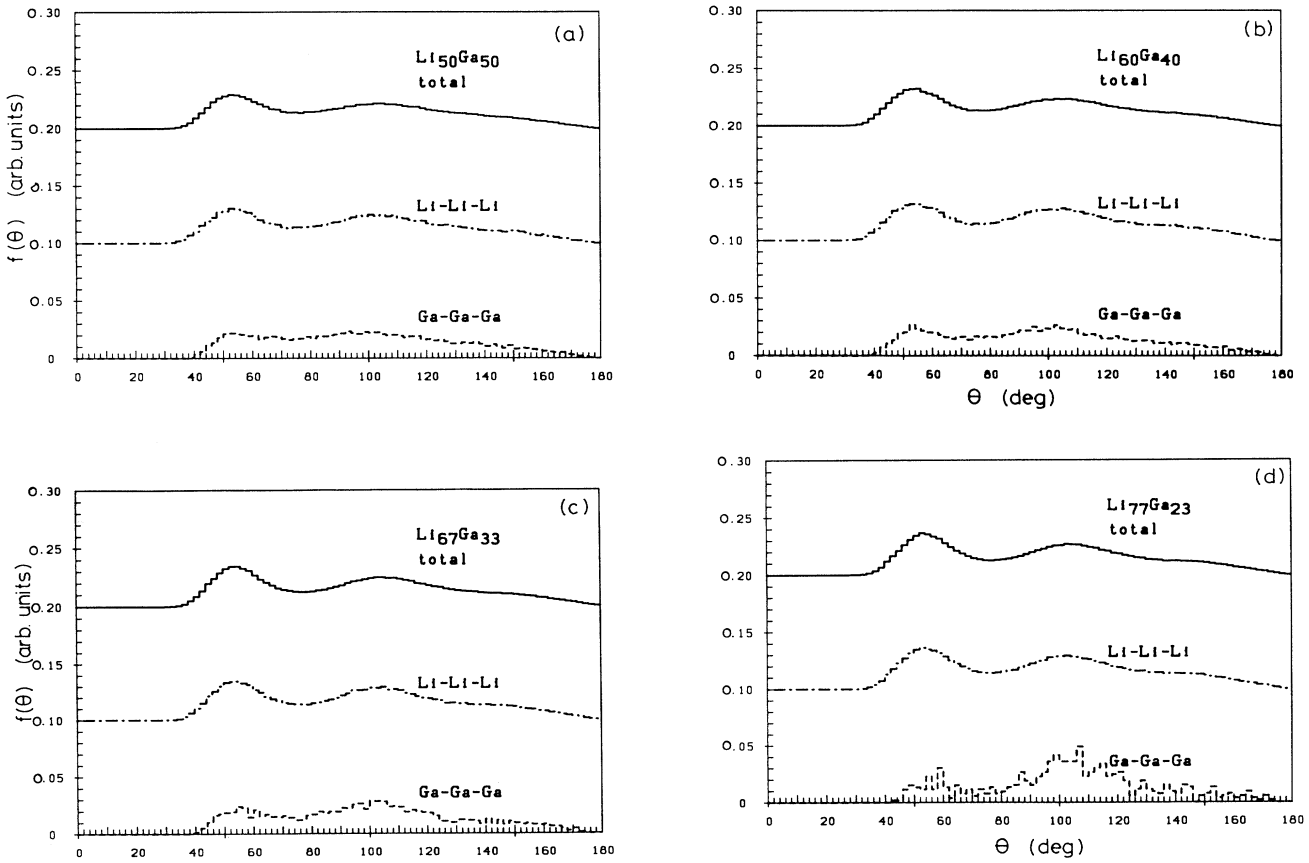


FIG. 9. Total and partial bond-angle distribution functions $f(\theta)$ in liquid Li-Ga alloys: (a) $Li_{0.50}Ga_{0.50}$, (b) $Li_{0.60}Ga_{0.40}$, (c) $Li_{0.67}Ga_{0.32}$, and (d) $Li_{0.77}Ga_{0.23}$.

tio $Q_p/Q_1$ of the positions of the prepeak and the main peak in $S_{\text{Ga-Ga}}(q)$ is almost exactly the same as between the first two peaks in the structure factors of the polyvalent elements (Table V). In both the Li-Ga alloys and the polyvalent elements, the position of the second peak almost exactly coincides with $2k_F$. This indicates that, in both cases, the stabilizing mechanism is the modulation of the random arrangement of the atoms by the Friedel modulations in the potential; and this appears to be a natural interpretation of the Zintl principle.

The most direct evidence comes perhaps from computergraphics: Fig. 11 shows a projection of a slice (about two bond lengths thick) of an instantaneous configuration of $Li_{77}Ga_{23}$. Ga-Ga bonds between nearest neighbors are drawn. We find that the majority of Ga atoms are part of Ga chains embedded in a Li matrix.

Finally, we compare our computer-simulation results with the neutron-diffraction data of Reijers *et al.*[8] for $Li_{50}Ga_{50}$ and for the zero-alloy $Li_{77}Ga_{23}$ (Fig. 12). For the zero alloy [where a diffraction experiment measures only the concentration fluctuations, i.e., $S(q)=S_{CC}(q)$] we find a reasonably good agreement between theory and experiment. For $Li_{50}Ga_{50}$, the first peak due to the concentration fluctuations is shifted to larger wave numbers compared to the diffraction experiment. The peak in $S_{NN}(q)$ contributes only with a small weight ($w_{NN}=0.22$, $w_{NC}=1.66$ $w_{CC}=3.11$), it is located close to $q=2.85$ Å$^{-1}$ in both theory and experiment. The neutron-weighted radial distribution functions (RDF) are shown in Fig. 13. For the zero alloy we find a distinct negative minimum in the RDF at $R_1=2.9$ Å) expressing the chemical short-range order. Beyond about $R\simeq 3.5$ Å, the RDF is essentially zero, so that the ordering does not extend beyond the nearest-neighbor shell. For the equiatomic alloy the RDF shows the peaks in the density-correlation functions, which are reasonably well reproduced by the simulation. Thus, the most serious difference between experiment and simulation is that the simulation predicts somewhat too short Li-Ga distances: this explains the shift in the negative peak in the RDF and the shift of the first peak in $S_{CC}(q)$. The shift in $S_{CC}(q)$ is, in addition, enhanced by the relatively large width of the main peak in the Ga-Ga structure factor.

Reijers *et al.* have speculated that the small ratio $Q_p/Q_1\sim 0.50$ might indicate the existence of polyanionic Ga clusters similar to those found in the liquid I-IV compounds of the heavy alkali metals where similar values of this quantity have been observed. $Q_p/Q_1\sim 0.5$ has also

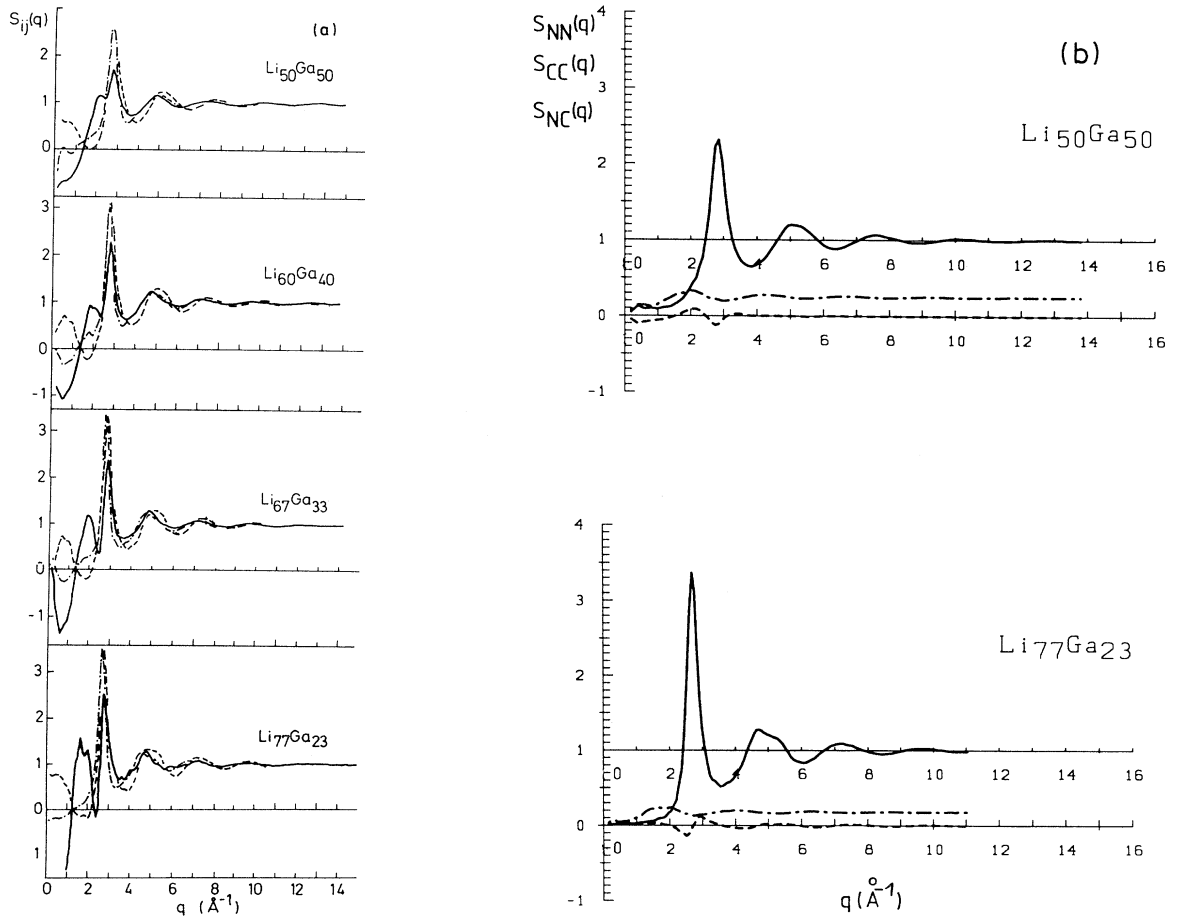


FIG. 10. Partial static structure factors $S_{ij}(q)$ ($i,j$=Li,Ga) (for key see Fig. 8) (a) and Bhatia-Thornton structure factors $S_{NN}(q)$ (solid line), $S_{NC}(q)$ (dashed line), and $S_{CC}(q)$ (dot-dashed line) (b) for Li-Ga alloys.

been found in liquid Cs-Sb alloys and interpreted as indicating the existence of polyanionic Sb chains.[69] Our calculations tend to confirm the existence of such loosely defined polyanionic clusters, but they also show that the ratio $Q_p/Q_1$ is not a very critical indicator for the existence of well-defined structural units.

## V. ELECTRONIC STRUCTURE OF LIQUID ALLOYS

The electronic structure of the molten alloys has been calculated using the LMTO-supercell technique. A detailed discussion of the method has been given in our papers on the electronic structure of the pure liquid metals.[28,70,71] The calculation is based on instantaneous

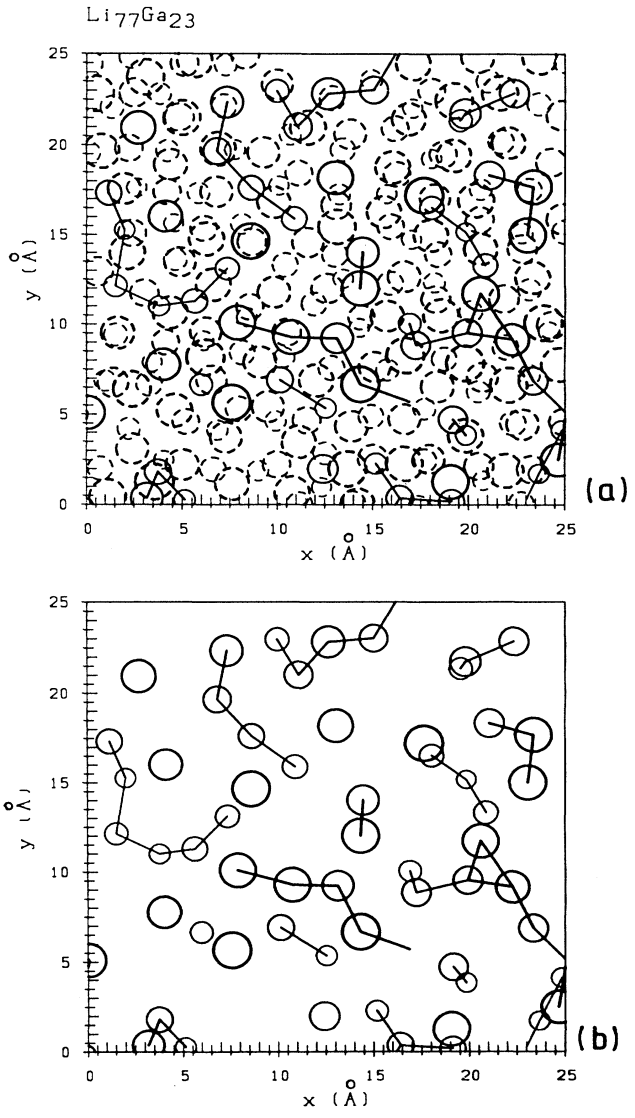


FIG. 11. (a) Projection of part of an instantaneous configuration of a 1000-atom model of $Li_{77}Ga_{23}$ on the $x,y$ plane. Solid circles, Ga; open circles, Li. The size of the symbols scales with the $z$ coordinate. Nearest-neighbor Ga-Ga bonds are drawn. (b) Shows the same configuration with the Li-atoms omitted.

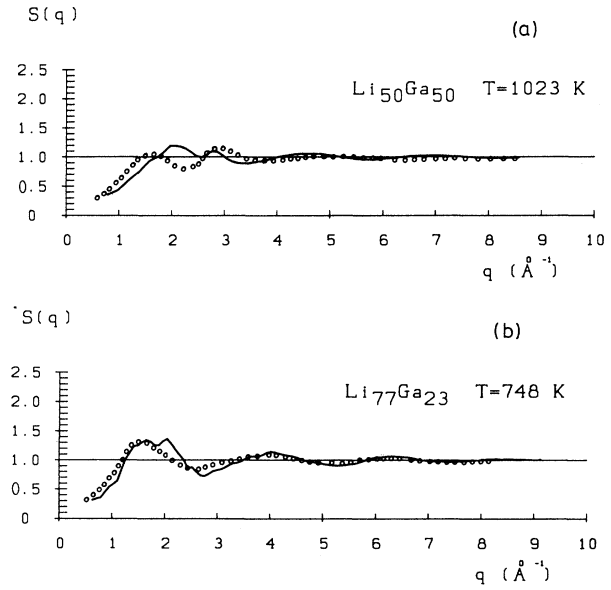


FIG. 12. Neutron-diffraction intensities for (a) $Li_{0.50}Ga_{0.50}$ and (b) $Li_{0.77}Ga_{0.23}$. Solid line, simulation; circles, experiment (Ref. 8).

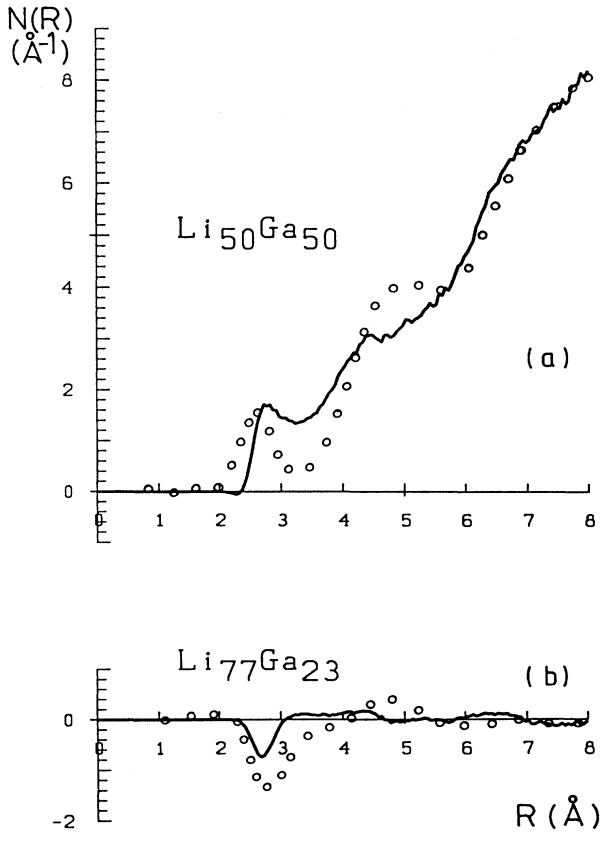


FIG. 13. Neutron-weighted radial distribution functions for (a) $Li_{0.50}Ga_{0.50}$ and (b) $Li_{0.77}Ga_{0.23}$. Solid line, simulation; circles, experiment (Ref. 8).

configurations of ensembles of 64 atoms enclosed in a periodically repeated cubic box. By comparing the pair-correlation functions of the 64-atom model with the results of the molecular-dynamics (MD) runs for the 1000-atom ensemble, we find that even such a small model reproduces the essential features of the liquid structure.

The total, partial, and angular-momentum decomposed densities of state for liquid $Li_{0.50}Ga_{0.50}$ and $Li_{0.77}Ga_{0.23}$ alloys are shown in Figs. 14 and 15. The result for the equiatomic alloy shows that the strong $sp^3$ hybridization characteristic for the crystalline Zintl phase is destroyed on melting. In the liquid alloy we find a deep pseudogap about 3 eV below the Fermi level separating a band of pure $s$ character on the Ga sites from a band of pure $p$ character on the Ga sites. The Li contribution to the DOS has a strongly mixed angular-momentum character, indicating that the electron states are in reality Ga states. Thus, the electronic DOS of molten $Li_{0.50}Ga_{0.50}$ is very similar to that of liquid Ge and we are led to the conclusion that, in the Zintl phases as well as in the elemental semiconductors, thermal disorder destroys the directed bonds associated with the formation of $sp^3$ hybrids. The DOS of the molten alloy resembles more closely that of the CsCl phase.

In the Li-rich alloy (Fig. 15) we again find a Ga $s$ band at higher binding energies (containing exactly two electrons per Ga atom), separated by a pseudogap from a $p$ band close to the Fermi level. This was also the situation in the crystalline $Li_3Ga_2$ and $Li_2Ga$ phases (see Figs. 4 and 5). The main difference between the liquid and the crystalline phases appears in the $s$ band. In the liquid phase the splitting of the $s$ band [which is a consequence of the back bonds between Ga atoms in different layers (chains) in the As-type (Se-type) Ga sublattices in $Li_3Ga_2$ and $Li_2Ga$] has disappeared. This is again reminiscent of

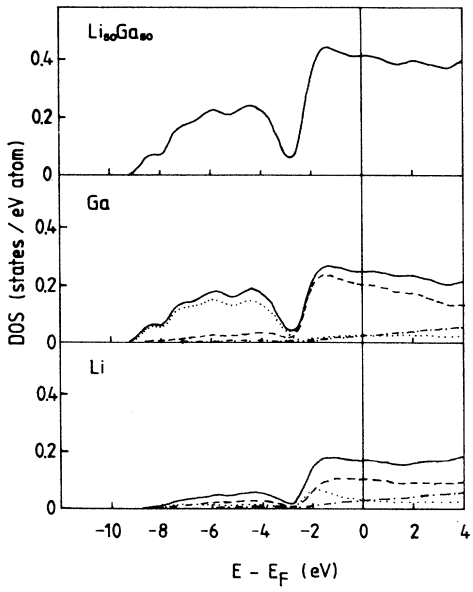


FIG. 14. Total, partial, and angular-momentum-decomposed electronic density of states for liquid $Li_{0.50}Ga_{0.50}$. For key, see Fig. 3.

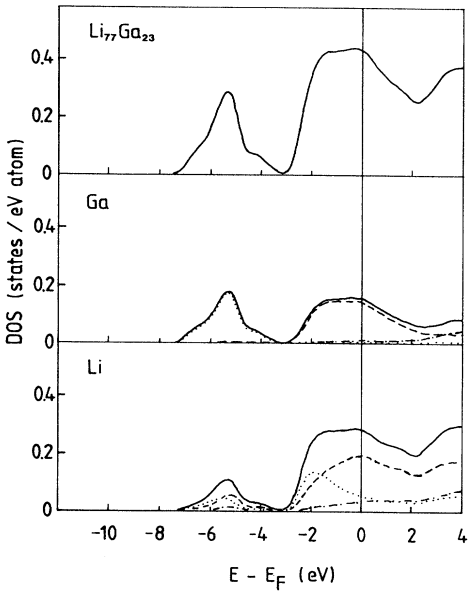


FIG. 15. Total, partial, and angular-momentum-decomposed electronic density of states for liquid $Li_{0.77}Ga_{0.23}$. For key, see Fig. 3.

the situation in amorphous[18] and liquid[62] arsenic and in liquid and amorphous Se where thermal disorder leads to a strong reduction of the Peierls splitting in the $s$ band. It should be possible to verify these predictions by photoemission spectroscopy, and we hope that our work will stimulate such experiments.

Thus, the results of the electronic structure calculations confirm our interpretation of the MD results for the atomic structure: in the liquid Li-Ga alloys, structure and bonding are dominated entirely by the strong attractive Ga potential. The Ga-Ga bonds are very similar to those formed by the element with the same number of electrons per atom, counting all electrons in the conduction band of the alloy as belonging to Ga. However, the proper reference is now the liquid element: with increasing Li content the electronic DOS and the Ga-Ga structure factor in the alloy resemble the DOS and the $S(q)$ of liquid Ge, As, and Se.

## VI. CONCLUSIONS

Our investigations of the structural and electronic properties of crystalline and liquid Li-Ga alloys demonstrate the validity of an extended Zintl principle. The bonding is dominated by the strong potential of the Ga ions and may be described at least formally in terms of a complete electron transfer. The well-known equivalences $Ga^- \equiv Ge$, $Ga^{2-} \equiv As$, $Ga^{3-} \equiv Se$ are reflected in a Ge-, As-, and Se-like Ga sublattices of the compounds LiGa, $Li_3Ga_2$, and $Li_2Ga$, and in the Ge-, As-, and Se-like electronic structure. The extended Zintl principle is also valid in the liquid phase: in liquid $Li_{0.50}Ga_{0.50}$ we find that thermal disorder destroys the $sp^3$ hybridization associated with diamondlike bonds, but this is again exactly analogous to liquid Ge. In the liquid Li-rich alloys we find short-range Ga-Ga correlations which are similar to

those observed in liquid As and liquid Se. These conclusions are in reasonable, although not entirely quantitative, agreement with neutron-diffraction data. Consideration of three-body terms will be necessary to improve agreement between theory and experiment. Our conjectures on the local atomic order are supported by the result of electronic structure calculations. We hope that our predictions of the electronic spectra can soon be tested against experiments.

## ACKNOWLEDGMENTS

This work has been supported by the Fonds zur Förderung der wissenschaftlichen Forschung in Österreich under Project No. 7192. The numerical calculations have been performed on the IBM-3090-400VE of the Computer Center of the University of Vienna, supported by the European Academic Supercomputer Initiative (EASI).

[1]E. Zintl, J. Goubeau, and W. Dullenkopf, Z. Phys. Chem. A **154**, 1 (1931); E. Zintl and H. Kaiser, Z. Anorg. Allg. Chem. **211**, 113 (1933).

[2]W. Klemm and E. Bussmann, Z. Anorg. Allg. Chem. **319**, 297 (1963).

[3]W. Klemm, Proc. Chem. Soc. (London) **329**, 328 (1958).

[4]For a review see, e.g., W. van der Lugt and W. Geertsma, Can. J. Phys. **65**, 326 (1987).

[5]J. A. Meijer, G. B. Vinke, and W. van der Lugt, J. Phys. F **16**, 845 (1986).

[6]H. Redslob, G. Steinleitner, and W. Freyland, Z. Naturforsch. Teil A **27**, 587 (1982).

[7]H. Ruppersberg and H. Reiter, J. Phys. F **12**, 1311 (1982).

[8]H. T. J. Reijers, W. van der Lugt, and C. van Dijk, Physica B **144**, 404 (1987); M. L. Saboungi, R. Blomqvist, K. J. Volin, and D. L. Price, J. Chem. Phys. **87**, 2278 (1987).

[9]P. Lamparter, W. Martin, S. Steeb, and W. Freyland, J. Non Cryst. Solids **61+62**, 279 (1984).

[10]A. Petric, A. D. Pelton, and M. L. Saboungi, J. Chem. F **18**, 1473 (1988).

[11]M. Tegze and J. Hafner, Phys. Rev. B **39**, 8263 (1989).

[12]F. Springelkamp, R. A. de Groot, W. Geertsma, W. van der Lugt, and F. M. Mueller, Phys. Rev. B **32**, 2319 (1985).

[13]M. Tegze and J. Hafner, Phys. Rev. B **40**, 9841 (1989).

[14]J. Hafner, J. Phys.: Condens. Matter **1**, 1133 (1989); J. Non-Cryst. Solids **117+118**, 64 (1990).

[15]A. Pasturel, J. Hafner, and P. Hicter, Phys. Rev. B **32**, 5009 (1985).

[16]P. Villars and L. D. Calvert, *Pearson's Handbook of Crystallographic Data for Intermetallic Phases* (American Society for Metals, Metals Park, 1985), Vols. 1–3.

[17]H. G. von Schnering, W. Hönle, and G. Krogull, Z. Naturforsch. Teil B **34**, 1678 (1979).

[18]J. Robertson, Adv. Phys. **32**, 361 (1983).

[19]J. Robertson, Phys. Rev. B **27**, 6322 (1983).

[20]G. Steinleitner, W. Freyland, and F. Hensel, Ber. Bunsenges. **79**, 1186 (1975).

[21]J. A. Meijer and W. van der Lugt, J. Phys.: Condens. Matter **1**, 9779 (1989).

[22]R. Xu, R. Kinderman, and W. van der Lugt, J. Phys.: Condens. Matter **3**, 127 (1991).

[23]E. Zintl and G. Brauer, Z. Phys. Chem. B **20**, 245 (1933).

[24]W. Hückel, *Structural Chemistry of Inorganic Compounds* (Elsevier, Amsterdam, 1951), p. 829.

[25]P. C. Schmidt, Phys. Rev. B **31**, 5015 (1985).

[26]W. E. Christensen, Phys. Rev. B **32**, 207 (1985).

[27]J. Hafner and W. Weber, Phys. Rev. **33**, 747 (1986).

[28]W. Jank and J. Hafner, Phys. Rev. B **41**, 1497 (1990).

[29]I. Stich, R. Car, and M. Parrinello, Phys. Rev. Lett. **63**, 2240 (1989).

[30]J. Hafner and W. Jank, J. Phys.: Condens. Matter **1**, 4235 (1989).

[31]Q. M. Zhang, G. Chiarotti, A. Selloni, R. Car, and M. Parrinello, J. Non Cryst. Solids **117+118**, 930 (1990).

[32]J. P. Gaspard, C. Bergman, C. Bichara, R. Bellissent, P. Chieux, and J. Goffart, J. Non Cryst. Solids **97+98**, 1283 (1977).

[33]T. Itami, M. Shimoji, J. A. Meijer, and W. van der Lugt, J. Phys. F **18**, 2409 (1988).

[34]S. Takeda and S. Tamaki, J. Phys. Soc. Jpn. **58**, 1484 (1989).

[35]M. Kitajima and M. Shimoji, in *Liquid Metals 1976,* edited by R. Evans and D. A. Greenwood, IOP Proc. No. 30 (Institute of Physics, London, 1976), p. 226.

[36]H. T. J. Reijers, W. van der Lugt, J. B. van Tricht, W. A. H. M. Vlak, and W. S. Howells, J. Phys.: Condens. Matter **1**, 8609 (1989).

[37]S. Tamaki, Z. Phys. Chem. Neue Folge **156**, 537 (1988).

[38]T. Itami, M. Shimoji, and W. van der Lugt, J. Less-Common Metals **152**, 75 (1989).

[39]W. Müller and J. Stöhr, Z. Naturforsch. Teil B **32**, 631 (1977).

[40]A compound $Li_5Ga_4$ has been reported by J. Stöhr, Z. Allg. Anorg. Chem. **474**, 221 (1981); see also P. Villars and L. D. Calvert (Ref. 16), but is not reported in the phase diagram of T. Itami, M. Shimoji, and W. van der Lugt, (Ref. 38).

[41]L. Bosio, A. Defrain, H. Curien, and A. Rimsky, Acta Crystallogr. B **25**, 995 (1969).

[42]C. Belin and R. G. Ling, J. Solid State Chem. **45**, 290 (1982); **48**, 40 (1983).

[43]B. F. Decker and J. S. Kasper, Acta Crystallogr. **12**, 503 (1959).

[44]H. L. Skriver, in *The LMTO Method,* Vol. 41 of *Springer Series in Solid State Sciences,* edited by P. Fulde (Springer, Berlin, 1984).

[45]O. K. Andersen, O. Jepsen, and D. Glötzel, in *Highlights of Condensed Matter Theory,* edited by F. Bassani, F. Fumi, and M. P. Tosi (North-Holland, Amsterdam, 1985).

[46]U. von Barth, L. Hedin, and J. F. Janak, Phys. Rev. B **12**, 1257 (1975).

[47]O. Jepsen and O. K. Andersen, Solid State Commun. **9**, 1763 (1971); G. Lehmann and M. Taut, Phys. Status Solidi B **54**, 469 (1972).

[48]Z. Pawlowska, N. E. Christensen, S. Satpathy, and O. Jepsen, Phys. Rev. B **43**, 7080 (1986); **59**, 1002 (1990).

[49]A. Ikawa and M. Fukutome, J. Phys. Soc. Jpn. **58**, 4517 (1989).

[50]S. Susman and T. O. Brun, Solid State Ionics, **5**, 413 (1981).

[51]M. Tegze and J. Hafner, J. Phys.: Condens. Matter **1**, 8293 (1989).

[52]X. Q. Guo, R. Podloucky, and A. J. Freeman, Phys. Rev. B **42**, 10912 (1990).

[53]J. Hafner, in *From Hamiltonians to Phase Diagrams,* Vol. 70 of *Springer Series in Solid State Sciences,* edited by P. Fulde

(Springer, Berlin, 1987).
[54]V. Heine and J. Hafner, in *Many Atom Interactions in Solids,* Vol. 48 of *Springer Proceedings in Physics,* edited by R. M. Nieminen, M. J. Puska, and M. J. Manninen (Springer, Berlin, 1990), p. 12.
[55]J. Hafner, J. Phys. F **15**, L43 (1985); in *From Hamiltonians to Phase Diagrams* (Ref. 53), p. 149ff.
[56]J. C. Phillips, *Covalent Bonding in Crystals, Molecules, and Polymers* (University of Chicago, Chicago, 1970).
[57]J. Friedel, J. Phys. (Paris) **39**, 651 (1978); **39**, 671 (1978).
[58]A. Arnold, N. Mauser, and J. Hafner, J. Phys.: Condens. Matter **1**, 965 (1989).
[59]J. Hafner, Phys. Rev. Lett. **62**, 648 (1990).
[60]J. Hafner, J. Phys.: Condens. Matter, **2**, 1271 (1990).
[61]P. B. Littlewood, Crit. Rev. Solid State Mater. Sci. **11**, 229 (1983).
[62]X. P. Li, P. B. Allen, R. Car, M. Parrinello, and J. Q. Broughton, Phys. Rev. B **41**, 3260 (1990).
[63]J. Hafner and M. C. Payne (unpublished).
[64]V. Heine and D. Weaire, Solid State Phys. **24**, 247 (1970).
[65]G. L. Krasko and A. B. Maknovetskii, Phys. Status Solidi B **66**, 349 (1974).
[66]A. B. Maknovetskii and G. L. Krasko, Phys. Status Solidi B **80**, 341 (1977).
[67]A. Arnold and N. Mauser, Comput. Phys. Commun. **59**, 267 (1990).
[68]H. Ruppersberg and W. Speicher, Z. Naturforsch. Teil A **31**, 47 (1976).
[69]P. Lamparter, W. Martin, and S. Steeb, J. Non-Cryst. Solids **61+62**, 279 (1984).
[70]W. Jank and J. Hafner, Phys. Rev. B **42**, 6926 (1990).
[71]W. Jank and J. Hafner, J. Phys.: Condens. Matter, **2**, 5065 (1990).